Involvement of caveolin-2 in caveolar biogenesis in MDCK cells

Ulla Lahtinen[a,1], Masanori Honsho[a], Robert G. Parton[b], Kai Simons[a], Paul Verkade[a,*]

[a] *Max-Planck-Institute of Molecular Cell Biology and Genetics, Pfotenhauerstrasse 108, 01307 Dresden, Germany*
[b] *Institute for Molecular Bioscience, University of Queensland, Centre for Microscopy and Microanalysis, and School of Biomedical Sciences, The University of Queensland, Brisbane, QLD 4072, Australia*

Received 18 December 2002; revised 29 January 2003; accepted 29 January 2003

First published online 13 February 2003

Edited by Felix Wieland

Abstract Caveolins have been identified as key components of caveolae, specialized cholesterol-enriched raft domains visible as small flask-shaped invaginations of the plasma membrane. In polarized MDCK cells caveolin-1 and -2 are found together on basolateral caveolae whereas the apical membrane, where only caveolin-1 is present, lacks caveolae. Expression of a caveolin mutant prevented the formation of the large caveolin-1/-2 hetero-oligomeric complexes, and led to intracellular retention of caveolin-2 and disappearance of caveolae from the basolateral membrane. Correspondingly, in MDCK cells over-expressing caveolin-2 the basolateral membrane exhibited an increased number of caveolae. These results indicate the involvement of caveolin-2 in caveolar biogenesis.

Key words: Caveolin-1; Caveolin-2; Caveola; MDCK

1. Introduction

Besides being components of apical and basolateral transport carriers [1–4], caveolin-1 and -2 have also been identified as structural components of caveolae [4–7]. Caveolins and caveolae have been implicated in a number of cellular processes including signal transduction, cholesterol homeostasis and transport [4,8–14]. In MDCK cells, caveolin-1 is present in both the apical and basolateral plasma membrane domains, whereas the expression of caveolin-2 is restricted to the basolateral membrane. There, caveolin-1 and -2 are found in caveolae [4]. Shortly after their synthesis in the endoplasmic reticulum, the caveolins assemble into caveolin-1 homo-oligomers and caveolin-1/-2 hetero-oligomers. During their transit through the Golgi complex [4,7] the oligomers increase in size [15] and become incorporated in special membrane domains termed rafts [13]. The oligomeric complexes segregate in the *trans*-Golgi network, where caveolin-1 homo-oligomers are sorted into the apical transport carriers, and the caveolin-1/-2 hetero-oligomers are directed to the basolateral route [4]. Several caveolin truncation mutants have recently been created in order to analyze the targeting of caveolins and also to find potential mutants inhibiting caveolin function [16,17]. One of the characterized mutants, caveolin-3-DGV-HA (DGV), lacks the 53 N-terminal amino acids upstream of the scaffolding domain. This mutant was used to analyze the role of caveolins in caveolar biogenesis in polarized MDCK cells.

2. Materials and methods

2.1. Cell culture

MDCKII cells were grown on 12 or 24 mm diameter Transwell filters for 2–3 days prior to use as described previously [18]. For MDCK cells stably expressing c-myc-tagged caveolin-2 (clone 54 [4]) 0.5 mg/ml G-418 was added to the medium.

2.2. Construction of recombinant Cav-3-DGV-HA adenovirus and adenoviral infections

The cDNA of caveolin-3-DGV-HA [16] was transferred from pCB6 vector to pShuttle-CMV vector using *Kpn*I and *Xba*I restriction sites, and recombinant adenovirus was constructed and propagated in 293 cells as described [19]. MDCK cells grown on 12 mm filters were infected with recombinant adenovirus from the apical side in 200 μl volume of infection medium (MEM supplemented with 0.2% bovine serum albumin and 20 mM HEPES, pH 7.4). For 24 mm diameter filters 1 ml of infection medium was used. After 12 h incubation, the infection medium was replaced by growth medium and the cells were used for experiments 3 days post infection.

2.3. Antibodies

Polyclonal anti-caveolin-1 (N-20) and anti-HA tag antibodies (HA probe) were from Santa Cruz. Monoclonal anti-HA antibodies were ammonium sulfate precipitated from hybridoma C12A5 supernatant. Anti-caveolin-2 antibodies (#1825) have been described previously [4]. Secondary FITC- or TRITC-conjugated antibodies were purchased from Jackson ImmunoResearch.

2.4. Immunofluorescence and quantitation

Immunofluorescent labelling was performed as described [4] and the cells were viewed under a Zeiss LSM410 confocal microscope. To quantitate the difference in fluorescent signal between control and DGV-expressing cells, samples with 50% infection frequency were used. The original x,y-images were opened in NIH image, rendering fluorescence values from 0 to 256. The fluorescence intensity at the basolateral membrane was measured at five rectangular sites of DGV-expressing or control cells. From the same cells the mean apical fluorescence was measured at a different z-plane. Measurements were performed on at least 15 cells from each group. Statistical differences were tested using a Student's t-test or a Welch test if the variances of the groups were not equal. Differences between groups were called statistically significant when $P < 0.05$.

2.5. Biochemical assays

Metabolic labelling of cells was carried out for 18 h with 300 μCi [^{35}S]methionine per 3 cm dish, whereafter the cells were solubilized and the samples were immunoprecipitated and subjected to gel electrophoresis as described [4]. Isoelectric focusing was performed as described [1]. Sucrose velocity gradient centrifugation in SDS–Triton X-100 was performed as described [4].

*Corresponding author. Fax: (49)-351-2101689.
E-mail address: verkade@mpi-cbg.de (P. Verkade).

[1] Present address: Folkhälsan Institute of Genetics and Department of Medical Genetics, University of Helsinki, Biomedicum Helsinki, Haarmaninkatu 8, 00290 Helsinki, Finland.

0014-5793/03/$22.00 © 2003 Published by Elsevier Science B.V. on behalf of the Federation of European Biochemical Societies.
doi:10.1016/S0014-5793(03)00135-2

2.6. Electron microscopy and quantitation of caveolae

MDCK cells were fixed with 2.5% glutaraldehyde in 0.1 M cacodylate buffer and processed for Epon embedding and electron microscopy according to standard protocols (see e.g. [20]). For quantitation of the number of caveolae, filters with an infection frequency of >95% were analyzed. Caveolae were recognized by their 50–80 nm flask-shaped structure as described [8,21]. The number of caveolae per μm plasma membrane length was calculated following the criteria described previously [22]. A general difference between control, DGV-expressing and caveolin-2-over-expressing cells was tested using a one-factor ANOVA test. Differences between specific cell types were tested using a Welch test since the variances between the groups were not equal. Differences between groups were called statistically significant when $P < 0.05$.

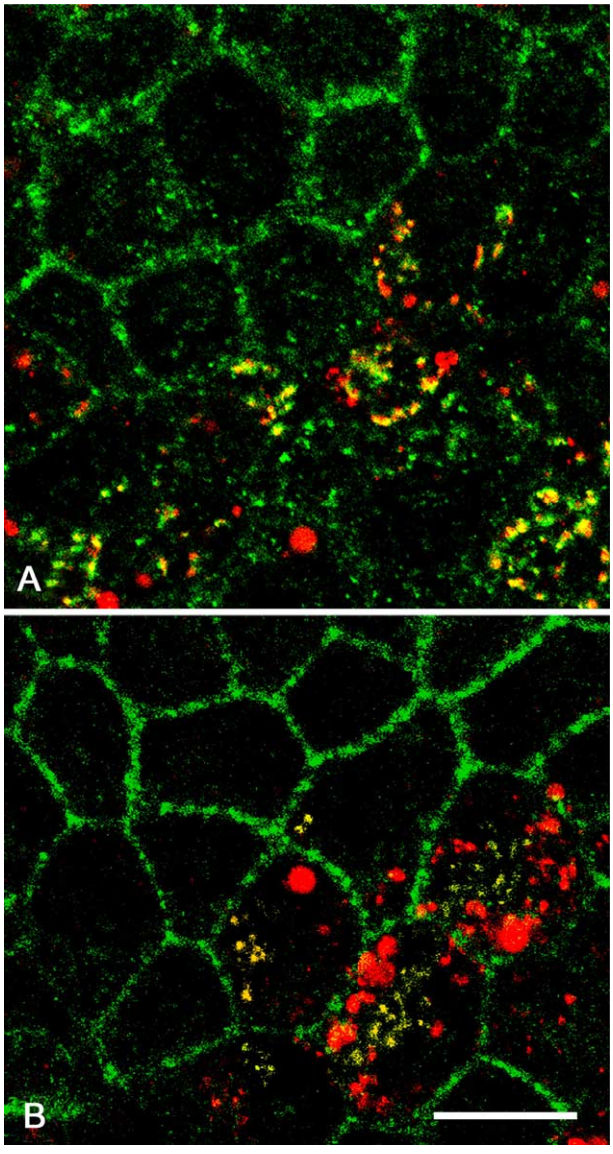

Fig. 1. Caveolin-2 accumulates intracellularly upon DGV expression in polarized MDCK cells. Immunofluorescence micrographs of polarized MDCK cells infected with recombinant DGV adenovirus at 50% infection frequency. In DGV-expressing cells (red in A and B) caveolin-2 (A, green) was completely retained intracellularly and partially co-localized with DGV. The distribution of caveolin-1 (B, green) was slightly affected. In addition to the plasma membrane some internal staining partially co-localizing with DGV was detected. Scale bar = 10 μm.

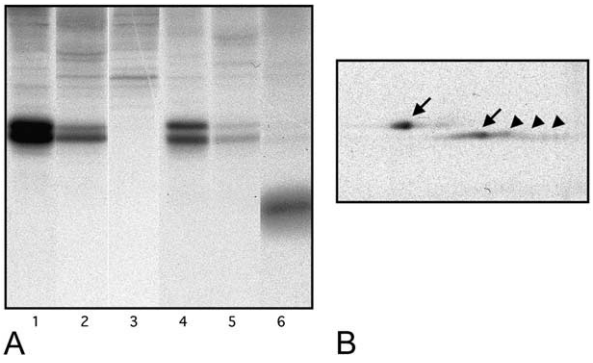

Fig. 2. Caveolin-1 and -2 co-precipitate with DGV. Control and DGV-expressing cells were metabolically labelled and lysed in the presence of Triton X-100 and SDS. A: In control cells, caveolin-1 (lane 1) and caveolin-2 antibodies (lane 2) precipitated characteristic caveolin doublets while HA antibodies did not precipitate any specific proteins (lane 3). In DGV-expressing cells, the caveolin doublets were precipitated with caveolin-1 (lane 4) and caveolin-2 (lane 5) antibodies, but both failed to co-precipitate any low molecular weight proteins corresponding to DGV. HA tag antibodies weakly co-precipitated the caveolin doublet (lane 6). This doublet was further resolved by two-dimensional electrophoresis and could be identified as caveolin-1 (arrows) and caveolin-2 (arrowheads) (B).

3. Results and discussion

The caveolin mutant DGV has recently been described to localize to the Golgi complex and distinct lipid droplets after transfection into BHK cells [16,17]. We constructed a recombinant adenovirus encoding DGV in order to control the frequency and level of expression. Consistent with previous data [17] DGV was localized in the perinuclear region corresponding to the Golgi complex and lipid droplets in polarized MDCK cells (Fig. 1). As described previously [4] caveolin-1 was detected at both the apical and basolateral plasma membrane while caveolin-2 was restricted to the basolateral membrane in control cells (Fig. 1B,A, respectively). In DGV-expressing cells, caveolin-2 was surprisingly not detectable at the plasma membrane but retained intracellularly. As in BHK cells [17], it co-localized to a large extent with DGV in the perinuclear region (Fig. 1A). The localization of caveolin-1 in DGV-expressing cells did not differ significantly from control cells (Fig. 1B). In addition to the plasma membrane staining only some intracellular staining of caveolin-1 co-localizing with DGV was visible (Fig. 1B). When the fluorescent signal for caveolin-1 at the apical membrane was quantified no difference between control and DGV-infected cells was detected (135.9 ± 3.1 vs. 134.6 ± 1.4 respectively, arbitrary IF units, mean ± S.E.M.). At the basolateral membrane the signal was reduced from 132.4 ± 4.7 to 64.3 ± 1.6 IF units. Whether this intracellular retention of caveolin-1 and -2 was due to direct protein–protein interactions with DGV was addressed by immunoprecipitation experiments. Caveolin-1 and caveolin-2 antibodies precipitated characteristic protein doublets corresponding to both caveolins in control cells (Fig. 2A, lanes 1 and 2) [4]. These caveolin doublets were similarly precipitated from DGV-expressing cells (Fig. 2A, lanes 4 and 5). DGV could not be detected co-precipitating with either caveolin-1 or -2 antibodies. When DGV was immunoprecipitated by means of its HA tag, small amounts of a doublet corresponding to the migration of the endogenous caveolins co-precipitated (Fig. 2A, lane 6). When this complex was further ana-

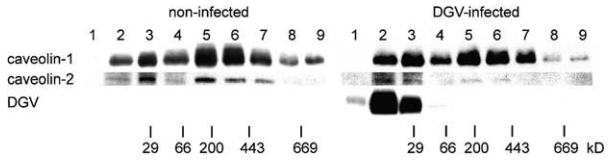

Fig. 3. Caveolin-2 oligomerization state is disturbed by DGV expression. Immunoblots of sucrose density gradient fractions of control and DGV-expressing cells probed with antibodies against caveolin-1, caveolin-2 and the HA tag of DGV. The corresponding molecular mass standards are indicated at the bottom. Caveolin-1 was found in both control and DGV-expressing cells in sizes ranging from the monomer size of 21 kDa up to high molecular weight oligomers of over 600 kDa. In control cells, caveolin-2 was mainly found in oligomers with a size of approximately 400 kDa. After infection with DGV most of the caveolin-2 was found in low molecular weight oligomers or in the size range of monomers. DGV was only found in the low molecular weight range corresponding to monomers or dimers.

lyzed by two-dimensional gel electrophoresis, it was resolved to spots representing both caveolin-1 and -2 (Fig. 2B) [4]. The DGV protein itself was not resolved in isoelectric focusing gels. Sucrose velocity gradient centrifugation was then used to analyze whether the DGV peptide becomes incorporated into the caveolin complexes and whether DGV expression altered the oligomerization state of the endogenous caveolins. Caveolin-1 and caveolin-2 were found in large oligomers in control cells (Fig. 3). In DGV-expressing cells, the amount of the high molecular weight oligomers of caveolin-2 was reduced and most of the protein now co-migrated with the DGV peptide as lower molecular weight oligomers or monomers (the DGV peptide having a calculated molecular weight of 12.5 kDa). High molecular weight caveolin-1 homo-oligomers appeared to be unaffected by DGV expression (Fig. 3). After immunoprecipitation with caveolin-1 antibodies the same amounts of caveolin-2 were left in the supernatant (not immunoprecipitated) of DGV-infected cells as in control cells (data not shown), indicating that the process of hetero-oligomerization between caveolin-1 and -2 was not disturbed. Together these data suggested that the caveolin-1/-2 hetero-oligomers could not progress into assembling the high molecular weight complexes. Impaired complex formation might prevent their exit from the Golgi complex and result in intracellular retention [4,23]. In immunoprecipitation experiments the exposure of epitopes and their accessibility for antibodies, or weak protein–protein interactions, may have been restricting for quantitative recovery, and the amount of caveolin-1/-2 co-precipitating with DGV could have been underestimated. Yet, considering the low amounts of caveolins co-precipitating with DGV, a direct interaction of DGV with the caveolins seemed unlikely to be the major cause of these effects. We also did not find any indications (e.g. by addition of exogenous cholesterol, changes in cholesterol distribution, or effects on transport (data not shown)) that DGV would cause a disturbance of cholesterol homeostasis as shown before [17,24].

Since caveolins are known to be involved in the formation of caveolae [25,26] we quantitated the number of caveolae. Approximately 1 caveola per μm membrane length was detected in control cells while in DGV-expressing cells, where caveolin-1 was still present at the basolateral membrane, the number of caveolae was drastically reduced (Fig. 4). The potential of caveolin-1 alone to form caveolae has been shown by expression of caveolin-1 in caveolae-lacking lymphocytes [25] and by the induction of caveolae on the apical membrane upon cross-linking of raft proteins in MDCK cells [27]. However, our current results demonstrate that the caveolin-1/-2 hetero-oligomeric complex is mainly involved in the formation of basolateral caveolae in MDCK cells. This is further substantiated by the fact that the number of caveolae in a caveolin-2-over-expressing cell line was significantly increased compared to the control cells (Fig. 4B). Interestingly, expres-

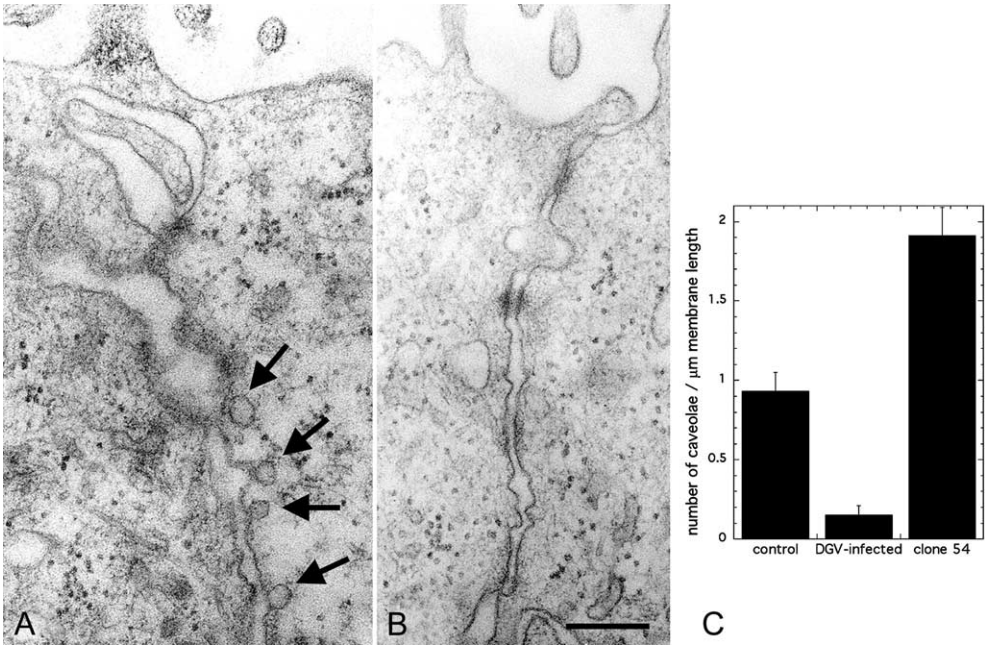

Fig. 4. Intracellular retention of caveolin-2 causes the disappearance of caveolae from the basolateral plasma membrane. Electron micrographs of ultrathin Epon sections of control cells show the basolateral localization of caveolae (arrows) (A) and the almost complete absence of caveolae in DGV-expressing cells (B). Scale bar = 250 nm. C shows the quantitation of the number of caveolae in control, DGV-expressing, and caveolin-2-over-expressing MDCK cells (clone 54).

sion of caveolin-1 alone in insect cells leads to the formation of 50–100 nm vesicular profiles while expression of both caveolin-1 and -2 leads to the formation of uniform 45–65 nm vesicular profiles [28]. Co-expression of caveolin-1 and -2 also leads to the formation of deeper caveolae in human fibroblasts than the expression of caveolin-1 alone [29]. We did not observe a change in size or shape of the caveolae in the caveolin-2-over-expressing cell line nor did we detect an induction of apical caveolae (not shown). This is most likely because caveolin-1 is also present in these cells and thus able to make hetero-oligomeric complexes. Recently a caveolin-2 knock-out mouse has been described [30]. Interestingly, in these mice caveolae are still present but they have severe lung disabilities similar to those described in caveolin-1 knock-out mice [26]. One of the notable findings in both the caveolin-1 knock-out mice, which lack caveolae, and the caveolin-2 knock-out mice is that both caveolin-2 and caveolin-1 levels are decreased [26,30]. Since it has been shown that the level of expression of caveolin is important for the formation of caveolae [25], analysis of the role of individual caveolins in these mice regarding the formation of caveolae is complicated. We therefore conclude that in MDCK cells caveolin-2 is a limiting or controlling factor for the biogenesis of basolateral caveolae at physiological caveolin-1 concentrations.

Acknowledgements: We thank Kim Ekroos and Beate Michel for cell culture, Patrick Keller for advice with the adenovirus system and Kurt Anderson for immunofluorescence quantitation. Masanori Honsho was partially supported by the Uehara memorial foundation.

References

[1] Wandinger-Ness, A., Bennett, M.K., Antony, C. and Simons, K. (1990) J. Cell Biol. 111, 987–1000.
[2] Kurzchalia, T.V., Dupree, P., Parton, R.G., Kellner, R., Virta, H., Lehnert, M. and Simons, K. (1992) J. Cell Biol. 118, 1003–1014.
[3] Glenney Jr., J.R. (1992) FEBS Lett. 314, 45–48.
[4] Scheiffele, P., Verkade, P., Fra, A.M., Virta, H., Simons, K. and Ikonen, E. (1998) J. Cell Biol. 140, 795–806.
[5] Rothberg, K.G., Heuser, J.E., Donzell, W.C., Ying, Y.S., Glenney, J.R. and Anderson, R.G. (1992) Cell 68, 673–682.
[6] Glenney, J.R. and Soppet, D. (1992) Proc. Natl. Acad. Sci. USA 89, 10517–10521.
[7] Scherer, P.E., Lewis, R.Y., Volonte, D., Engelman, J.A., Galbiati, F., Couet, J., Kohtz, D.S., van Donselaar, E., Peters, P. and Lisanti, M.P. (1997) J. Biol. Chem. 272, 29337–29346.
[8] Parton, R.G. (1996) Curr. Opin. Cell Biol. 8, 542–548.
[9] Kurzchalia, T.V. and Parton, R.G. (1999) Curr. Opin. Cell Biol. 11, 424–431.
[10] Smart, E.J., Graf, G.A., McNiven, M.A., Sessa, W.C., Engelman, J.A., Scherer, P.E., Okamoto, T. and Lisanti, M.P. (1999) Mol. Cell. Biol. 19, 7289–7304.
[11] Ikonen, E. and Parton, R.G. (2000) Traffic 1, 212–217.
[12] Schlegel, A. and Lisanti, M.P. (2001) J. Cell Physiol. 186, 329–337.
[13] Simons, K. and Ikonen, E. (1997) Nature 387, 569–572.
[14] Sotgia, F., Razani, B., Bonuccelli, G., Schubert, W., Battista, M., Lee, H., Capozza, F., Schubert, A.L., Minetti, C., Buckley, J.T. and Lisanti, M.P. (2002) Mol. Cell. Biol. 22, 3905–3926.
[15] Monier, S., Parton, R.G., Vogel, F., Behlke, J., Henske, A. and Kurzchalia, T.V. (1995) Mol. Biol. Cell 6, 911–927.
[16] Luetterforst, R., Stang, E., Zorzi, N., Carozzi, A., Way, M. and Parton, R.G. (1999) J. Cell Biol. 145, 1443–1459.
[17] Pol, A., Luetterforst, R., Lindsay, M., Heino, S., Ikonen, E. and Parton, R.G. (2001) J. Cell Biol. 152, 1057–1070.
[18] Pimplikar, S.W., Ikonen, E. and Simons, K. (1994) J. Cell Biol. 125, 1025–1035.
[19] He, T.C., Zhou, S., da Costa, L.T., Yu, J., Kinzler, K.W. and Vogelstein, B. (1998) Proc. Natl. Acad. Sci. USA 95, 2509–2514.
[20] Parton, R.G. (1995) J. Histochem. Cytochem. 43, 731–733.
[21] Parton, R.G. and Simons, K. (1995) Science 269, 1398–1399.
[22] Vogel, U., Sandvig, K. and van Deurs, B. (1998) J. Cell Sci. 111, 825–832.
[23] Machleidt, T., Li, W.P., Liu, P. and Anderson, R.G. (2000) J. Cell Biol. 148, 17–28.
[24] Roy, S., Luetterforst, R., Harding, A., Apolloni, A., Etheridge, M., Stang, E., Rolls, B., Hancock, J.F. and Parton, R.G. (1999) Nat. Cell Biol. 1, 98–105.
[25] Fra, A.M., Williamson, E., Simons, K. and Parton, R.G. (1995) Proc. Natl. Acad. Sci. USA 92, 8655–8659.
[26] Drab, M., Verkade, P., Elger, M., Kasper, M., Lohn, M., Lauterbach, B., Menne, J., Lindschau, C., Mende, F., Luft, F.C., Schedl, A., Haller, H. and Kurzchalia, T.V. (2001) Science 293, 2449–2452.
[27] Verkade, P., Harder, T., Lafont, F. and Simons, K. (2000) J. Cell Biol. 148, 727–739.
[28] Li, S., Galbiati, F., Volonte, D., Sargiacomo, M., Engelman, J.A., Das, K., Scherer, P.E. and Lisanti, M.P. (1998) FEBS Lett. 434, 127–134.
[29] Fujimoto, T., Kogo, H., Nomura, R. and Une, T. (2000) J. Cell Sci. 113, 3509–3517.
[30] Razani, B., Wang, X.B., Engelman, J.A., Battista, M., Lagaud, G., Zhang, X.L., Kneitz, B. and Hou Jr., H. (2002) Mol. Cell. Biol. 22, 2329–2344.